



Published in final edited form as:

Structure. 2015 September 1; 23(9): 1573–1583. doi:10.1016/j.str.2015.06.015.

## The structural role of antibody N-glycosylation in receptor interactions

Ganesh P. Subedi and Adam W. Barb\*

Roy J. Carver Department of Biochemistry, Biophysics and Molecular Biology, Iowa State University, Ames, IA 50011

### Abstract

Asparagine(N)297-linked glycosylation of IgG Fc is required for binding to Fc $\gamma$ RIIIa, IIb and IIIa though it is unclear how it contributes. We found the quaternary structure of glycosylated Fc was indistinguishable from aglycosylated Fc indicating N-glycosylation does not maintain relative Fc C $\gamma$ 2/C $\gamma$ 3 domain orientation. However, the conformation of the C'E loop, which contains N297, was significantly perturbed in the aglycosylated Fc variant. The conformation of the C'E loop as measured with a range of Fc variants shows a strong correlation with Fc $\gamma$ RIIIa affinity. These results indicate the primary role of the IgG1 Fc N-glycan is to stabilize the C'E loop through intramolecular interactions between carbohydrate and amino acid residues and preorganize the Fc $\gamma$ RIIIa interface for optimal binding affinity. The features that contribute to the capacity of the IgG1 Fc N-glycan to restrict protein conformation and tune binding affinity are conserved in other antibodies including IgG2-4, IgD, IgE and IgM.

### Introduction

Antibodies form a specific bridge between pathogens and the immune system to initiate a protective pro-inflammatory response. Immunoglobulin G (IgG) is the most abundant serum borne antibody and can trigger multiple pathways, including natural killer cell mediated antibody dependent cellular cytotoxicity (ADCC) (Janeway et al., 2008). The specificity afforded by tight binding interactions through the IgG fragment antigen binding (Fab) regions is leveraged by exogenous therapeutic monoclonal antibodies (mAbs) used in the treatment of a wide variety of diseases, including cancer, autoimmune disorders and transplant rejection, to name a few (Adams and Weiner, 2005; Chan and Carter, 2010; Scott et al., 2012; Singh et al., 2009; Sliwkowski and Mellman, 2013). These protective and curative effects largely require an intact IgG Fragment crystallizable (Fc) region for appropriate interaction with cell surface Fc  $\gamma$  receptors (Fc $\gamma$ Rs) (Bruhns et al., 2009; Jiang et al., 2011; Nimmerjahn and Ravetch, 2008; Siberil et al., 2007). It is well known that the co-translational modification of Fc with an asparagine(N)-linked carbohydrate chain (glycan) is required for Fc $\gamma$ R interactions (Arnold et al., 2007; Jefferis et al., 1998; Mimura et al., 2001;

\*corresponding author abarb@iastate.edu.

**Publisher's Disclaimer:** This is a PDF file of an unedited manuscript that has been accepted for publication. As a service to our customers we are providing this early version of the manuscript. The manuscript will undergo copyediting, typesetting, and review of the resulting proof before it is published in its final citable form. Please note that during the production process errors may be discovered which could affect the content, and all legal disclaimers that apply to the journal pertain.

Nose and Wigzell, 1983), but it is not known why. Appropriate N-glycosylation presents a significant barrier to mAb manufacture because less expensive microbial expression systems are incapable of appropriate N-glycosylation (Chadd and Chamow, 2001; Jaffe et al., 2014; Roque et al., 2004; Sethuraman and Stadheim, 2006).

Certain structural features of Fc are well characterized. Fc is a homodimer of the C-terminal half of the Ig  $\gamma$  heavy chain polypeptide. Fc forms a symmetric homodimer that is connected through non-covalent interactions and disulfide bonds. Fc retains full receptor binding properties once the Fab domains are removed by proteolysis (Franklin, 1975; Nisonoff et al., 1960; Porter, 1959). Each Fc heavy chain monomer consists of an N-terminal C $\gamma$ 2 domain that is linked by disulfide bonds in the hinge region to the corresponding C $\gamma$ 2 domain of the dimer (Figure 1). C $\gamma$ 3 domains form a large non-covalent dimer interface, further stabilizing the dimer conformation.

The C $\gamma$ 2 domains contain a single glycosylation site at N297, which resides at the tip of the C'E loop (Fig 1). The Fc N-glycan is primarily of a complex, biantennary type (Fig 1B) with the predominant forms containing 8 residues (Mizuochi et al., 1982). Though N-glycosylation is required for binding of the low affinity Fc $\gamma$ Rs (Jefferis, 2009; Lux et al., 2013), the primary interface between Fc and Fc $\gamma$ RIIIa is formed by polypeptide contacts and the receptor polypeptide does not directly contact the Fc N-glycan (Sondermann et al., 2000). It was likewise noted that changes to the N-glycan termini, distal to the site of the intermolecular polypeptide contacts by  $>20\text{\AA}$ , impact Fc $\gamma$ RIIIa affinity (Kaneko et al., 2006; Raju, 2008; Scallon et al., 2007; Yamaguchi et al., 2006). Intermolecular glycan-glycan contacts between Fc and the Fc $\gamma$ R have been observed by crystallography, but these are not required for binding and involve only the first few Fc N-glycan residues (Ferrara et al., 2011; Mizushima et al., 2011). Fc $\gamma$ RIIIa binds Fc with a 1:1 stoichiometry, breaking the symmetry of the Fc dimer and making contact with the C'E loop of one Fc C $\gamma$ 2 domain (Fig 1).

Fc structures solved by x-ray crystallography, with few exceptions, show a largely similar C $\gamma$ 2 domain orientation (reviewed in (Frank et al., 2014)). One hypothesis suggests the Fc N-glycan affects Fc $\gamma$ R binding by contributing to proper C $\gamma$ 2 domain orientation, particularly with respect to galactose-terminated and aglycosylated Fc (Borrok et al., 2012; Crispin et al., 2009; Frank et al., 2014; Krapp et al., 2003; Sondermann, 2013). This is supported by contacts of the N-glycans from each C $\gamma$ 2 domain at the Fc dimer symmetry axis, and indicates that removing the N-glycan would cause collapse of the C $\gamma$ 2 domains, rendering Fc incapable of binding Fc $\gamma$ Rs. This hypothesis was put in doubt by our recent report that Fc containing an N-glycan trimmed back to a single GlcNAc residue still bound Fc $\gamma$ R with reasonable affinity because this Fc glycoform does not contain enough residues to make the glycan-glycan contacts at the Fc dimer symmetry axis (Subedi et al., 2014). Furthermore, this study established a link between N-glycan motion and Fc $\gamma$ RIIIa affinity.

The N-glycan was resolved in the first Fc structure solved 40 years ago (Huber et al., 1976). Based on this evidence it was long suggested that the N-glycan binds tightly to the Fc polypeptide surface, however, significant motions of the N-glycan termini were recently observed (Barb and Prestegard, 2011). This observation led to a new hypothesis stating the

N-glycan influences Fc $\gamma$ R affinity through motion whereby a more mobile (less restricted) N-glycan is associated with weaker Fc $\gamma$ R affinity. Indeed, such a link was observed (Subedi et al., 2014). However, these studies were not capable of defining the mechanism by which the Fc N-glycan contributes to Fc $\gamma$ R affinity or creating a new link between the structure of a carbohydrate and activity of the protein to which it is attached.

Solution methods to characterize macromolecular structure open new windows into the conformation and conformational distribution sampled in a dilute medium (Ishima and Torchia, 2000; Lindorff-Larsen et al., 2005; Mertens and Svergun, 2010; Mittermaier and Kay, 2006). Solution nuclear magnetic resonance (NMR) spectroscopy excels with dynamic molecules or moieties that resist crystallization. The timescales of Fc N-glycan motion were described with these techniques (Barb and Prestegard, 2011). Extending NMR-based methods to measure the orientation of domains or local structural elements is capable of revealing conformations not visible in structures determined by x-ray crystallography. NMR fails to solve complete, all-atom structures with large molecules due to insufficient resolution of each peak and because of signal sapping line broadening effects that scale with molecule mass (Cavanagh et al., 2007; Tugarinov et al., 2004). However, targeted studies using selective labeling can reveal molecular features not visible through any other technique (Kato et al., 2010; Religa et al., 2010; Tugarinov et al., 2006). By combining the best aspects of solution and solid-state techniques we can characterize relationships between structure and activity with high precision.

In this study we evaluate the contribution of Fc N-glycosylation to Fc structure and Fc $\gamma$ RIIIa affinity to determine how the Fc N-glycan contributes to Fc activity, and in so doing, define the mechanism behind a previously unknown role for N-glycans in biology. We utilized two well-described Fc variants that are reported to show no measurable affinity for Fc $\gamma$ RIIIa: (glycosyl) Fc D265A (Baudino et al., 2008; Bournazos et al., 2014; Clynes et al., 2000; Lund et al., 1996; Lund et al., 1995) and (aglycosyl) Fc T299A (Lazar and Karki, 2009; Sazinsky et al., 2008; Subedi et al., 2014). Here we report the identification of IgG1 Fc features that are stabilized by N-glycosylation, and in the stabilized state contribute to Fc $\gamma$ RIIIa binding. These results are likewise informative of human IgG2-4, D, E and M because the structural elements surrounding the IgG1 Fc N-glycan, including location and potentially restricting residues, are conserved in these antibodies (Subedi et al., 2014).

## Results

### N-glycosylation effects on Fc quaternary structure

To probe the effects of glycosylation on Fc quaternary structure, we first measured the relative orientation of the Fc C $\gamma$ 2 and C $\gamma$ 3 domains using solution NMR spectroscopy. Using selectively  $^{15}\text{N}$ -amino acid enriched HEK293F cell expression medium we recovered high yields (30–50 mg/L) of appropriately glycosylated and  $^{15}\text{N}$ -labeled IgG1 Fc (see Fig S1). Sparse amino acid labeling provides peak separation and supports measurement of residual dipolar couplings (RDCs) to define the relative orientation of each observable N-H bond vector (Prestegard et al., 2014). If the structure of the individual C $\gamma$ 2 and C $\gamma$ 3 domains in solution mirrors the conformation of available models, RDCs can be interpreted to reveal the relative orientations of these two domains with high precision.

RDCs from [ $^{15}\text{N}$ -Y,K]-Fc wt were measured with high precision ( $-22 - +26 \pm 1.5$  Hz) and used to calculate alignment parameters from a range of Fc structures in the Protein Data Bank determined using x-ray diffraction data (Berman et al., 2002). Fc behaves as symmetric dimer in solution and a single peak for each amino acid is observed, even though two copies of the polypeptide are present. The quality of fit to each structure was quantified using a Q value (Cornilescu et al., 1998); Q values range from 0 – 1 with optimal values 0.2. Of the structures tested, 1L6X, generated using the highest-resolution Fc data available (1.65 Å (DeLano et al., 2000)), fit to the RDC dataset with  $Q=0.185$  which was lower than any other structure tested (Tables 1 & S1). This result is notable because it indicates the 1L6X model closely represents the dominant orientation of the individual  $C\gamma 2$  and  $C\gamma 3$  domains in solution, and thus, proposed alternative conformations must be populated only minimally (Frank et al., 2014). Q values represent changes in both local structure (the precise N-H vector orientation, for example) and global structure (relative domain orientations) and some structures derived by x-ray crystallography have imprecise local structural details. We eliminated the effect of local structural differences in our analysis by individually fitting the domain orientation of each PDB using the well-resolved domains from 1L6X to reveal a similar result, with only one model showing a slightly lower Q (3AY4, 0.183; Table 1). The Q value was improved to a value of 0.170 by small rotations of the  $C\gamma 2$  domain relative to the  $C\gamma 3$  domain.

RDCs reveal little difference between the predominant quaternary structures of an aglycosylated Fc variant in solution, Fc wt in solution, and Fc wt in the crystal lattice. The Fc T299A variant disrupts the N297-X-T299 Fc N-glycosylation sequon and is expressed without an N-glycan (Gavel and von Heijne, 1990). RDCs measured with Fc T299A were similar to Fc wt ( $R^2=0.94$ ) and also fit well to 1L6X with  $Q=0.177$  (Table S1), which improved to 0.170 by similar small rotations of the  $C\gamma 2$  domain. A comparison of  $C\gamma 2$  orientations, shown in Figure 2, reveals the high degree of similarity between the  $C\gamma 2$  orientations from crystallography and NMR. Thus, the effect of glycosylation on  $C\gamma 2$  orientation is restricted to small amplitudes or small populations not identified here. Based on these data it appears stabilization of the Fc  $C\gamma 2$  domain orientation is not the predominant contribution of N-glycosylation to Fc $\gamma$ RIIIa binding.

### N-Glycosylation stabilizes the Fc C' strand and C'E loop

Though the relative domain orientation appeared highly similar in the Fc wt and Fc T299A samples, a few key differences are found in  $^1\text{H}$ - $^{15}\text{N}$ -HSQC-TROSY spectra as shown in Figure 3 and 4A. The majority of the peaks corresponding to  $^{15}\text{N}$ -Y and  $^{15}\text{N}$ -K amide moieties do not change, however, Y300 shifts to a large extent in the Fc T299A spectrum, and Y296, usually not observed in Fc wt, is observed with Fc T299A. This is consistent with the observation of missing density for Q295 and Y296 in a structure of aglycosylated Fc solved by Georgiou and coworkers (Borrok et al., 2012). Two other residues, K288 and K290, also shift and indicate significant conformational rearrangement at these sites. The four residues identified in this experiment are connected to the same secondary structural element: the C'E loop. Y300 and Y296 are closest to the N297 site of N-glycosylation while K288 and K290 are found further up the C' strand that leads into the C'E loop (Fig 3B).

The changes in amide crosspeak positions are mirrored by changes in motion of the C'E loop. Solution NMR spectroscopy offers the capability to probe macromolecular motion to atomic detail by measuring rates of signal relaxation following 180° inversion (longitudinal relaxation,  $R_1$ ) or reorientation by 90° (transverse relaxation,  $R_2$ ) of the net nuclear magnetization vector relative to the external magnetic field. These relaxation rates are sensitive to motion as fast or faster than the ~20 ns Fc correlation time ( $R_1$  and  $R_2$ ) or motion in the microsecond to millisecond timescale ( $R_2$  only) (Barb and Prestegard, 2011; Cavanagh et al., 2007). We observed no clear changes in  $R_1$  relaxation rates for Fc secondary structural elements by comparing rates measures with Fc wt and Fc T299A, however, the  $R_2$  relaxation rate for the Y300 amide  $^{15}\text{N}$  nucleus was greater in the Fc T299A variant than the Fc wt protein (Fig 4B and Table S2). In total these data indicate the C'E loop experiences an increase in the effect of relatively slow microsecond to millisecond motion when the N-glycan was absent. Significant differences observed in C'E loop and C' strand conformation and nuclear relaxation rates suggest that the Fc N-glycan stabilizes Fc structure and contributes to Fc $\gamma$ RIIIa binding by stabilizing local conformation of the C'E loop, rather than by stabilizing global quaternary structure.

### C'E loop conformation correlates with Fc $\gamma$ RIIIa affinity

To this point we identified local structural differences between Fc with a complex-type N-glycan and aglycosylated Fc. We previously determined that Fc with a minimal N-glycan, consisting of only a single GlcNAc residue attached at N297 [also referred to as (1)GlcNAc-Fc wt], binds Fc $\gamma$ RIIIa with a 10-fold reduction in affinity when compared to Fc wt with a complex-type N-glycan as shown in Figure 5 (Subedi et al., 2014). This observation casts further doubt onto the idea that the N-glycan orients the C $\gamma$ 2 domains for optimal Fc $\gamma$ RIIIa binding because the majority of the N-glycan, and the proposed N-glycan/N-glycan contacts at the Fc dimer interface, cannot be formed in the (1)GlcNAc-Fc wt glycovariant (Baruah et al., 2012; Deisenhofer, 1981; Krapp et al., 2003; Sutton and Phillips, 1983). A published structure of (1)GlcNAc-Fc does not show essential contacts between the (1)GlcNAc and polypeptide residues due to poor electron density of the C'E loop (Baruah et al., 2012), an unfortunate result because the binding affinity of the (1)GlcNAc-Fc glycoform is intermediate (5  $\mu\text{M}$ ) between Fc wt (0.5  $\mu\text{M}$ ) and Fc T299A (>50  $\mu\text{M}$ ) and might highlight basic features of the Fc:Fc $\gamma$ RIIIa complex. Indeed, one striking structural difference is found in an  $^1\text{H}$ - $^{15}\text{N}$ -HSQC-TROSY spectrum that revealed a large displacement of the Y300 peak (Fig 5A).

The (1)GlcNAc residue shares a hydrophobic surface with the V264 sidechain and forms a hydrogen bond, through the acetamide moiety, with the D265 carboxylate (Fig 1C). If the hydrogen bond is important for stabilizing the C'E loop through the (1)GlcNAc residue, the D265A mutation should affect the position of the Y300  $^1\text{H}$ - $^{15}\text{N}$  crosspeak. It is well known that Fc D265A is glycosylated but fails to bind Fc $\gamma$ RIIIa (Clynes et al., 2000; Lund et al., 1995), consistent with our observation of weak binding with  $K_D > 50 \mu\text{M}$  (Figs 5 and S2). An  $^1\text{H}$ - $^{15}\text{N}$ -HSQC-TROSY spectrum reveals a significant shift of the Y300 peak in the D265A variant, further from that of the (1)GlcNAc Fc (Fig 5A). The assignment of the Y300 peak in the spectrum of Fc D265A was confirmed through further mutation (Fig 5B–D). The large shift of the Y300 crosspeak in Fc D265A is independent of glycoform (as

characterized in Figs S1,S3&S4), indicating the D265 coordination of the (1)GlcNAc residue is crucial for maintaining the C'E loop in the conformation observed with glycosylated Fc wt. Attempts to observe the conformation of the C'E loop in the Fc:Fc $\gamma$ RIIIa complex were unsuccessful due to line broadening relaxation, likely resulting from intermediate kinetic exchange of the complex on the NMR timescale (data not shown).

A line plotted through the overlaid Y300 peaks from wt and D265A Fcs with various glycoforms traces an arc across the spectra with substantial displacements in both dimensions (4.5 ppm  $^{15}\text{N}$ , 0.35 ppm  $^1\text{H}$ ). This large deviation indicates a large conformational alteration in C' strand and C'E loop conformation, and interestingly, the Y300 chemical shift in both the  $^{15}\text{N}$  and  $^1\text{H}$  dimensions correlates with Fc $\gamma$ RIIIa affinity as measured by surface plasmon resonance ( $R^2 = 0.96, 0.73$ ; respectively). This strong correlation supports the hypothesis that the Fc N-glycan contributes to Fc $\gamma$ RIIIa binding by restricting C'E loop conformation through glycan-polypeptide interactions.

### Interactions between the (1)GlcNAc residue and polypeptide stabilize the N-glycan

D265 stabilizes the N-glycan through a hydrogen bond with the (1)GlcNAc residue, therefore it is expected that a similar restriction may be observed with peaks corresponding to N-glycan residues. N-glycan residues can be specifically labeled by adding  $^{13}\text{C}_\text{U}$ -glucose to the expression medium (Yamaguchi et al., 1998).  $^1\text{H}$ - $^{13}\text{C}$  HSQC spectra of  $^{13}\text{C}$ -labeled Fc show clear signatures of N-glycan resonances and indicate that the majority of the observed  $^{13}\text{C}$  labels are located in glycan residues, likely due to the presence of amino acids in the serum-free expression medium that inhibit metabolic scrambling of the labels (Fig S5–S6).

Anomeric  $^1\text{H}$ - $^{13}\text{C}$  correlations are valuable probes of N-glycan structure because the resonance frequencies of these groups are distinct from the other carbohydrate correlations. The (1)-GlcNAc anomeric  $^1\text{H}1$ - $^{13}\text{C}1$  crosspeak is found separated from the remaining anomeric crosspeaks due to the unique N-linkage. It is surprising that this moiety, in all Fc wt glycoforms analyzed, gives rise to two components. One minor peak is observed with a resonance frequency of 5.1 ppm ( $^1\text{H}$ ), and another predominant peak was observed at 5.0 ppm ( $^1\text{H}$ ) as shown in Figure 6. This peak duplication indicates a slow conformational exchange of the atoms (on the NMR timescale) between two distinct chemical environments. Similar peak duplication is also observed for peaks corresponding to the 2, 3, and 6 positions of the (1)GlcNAc residue (Fig S7). The duplicated peaks collapse into a single crosspeak by either removing all tertiary structure by Fc proteolysis, or by removing the D265 carboxylate through amino acid substitution. The single crosspeak overlaps with the less intense signal in the Fc wt spectrum. This evidence indicates that a single environment of the (1)GlcNAc is consistent with proper C'E loop conformation and Fc $\gamma$ RIIIa binding.

It is tempting to conclude that the two peaks observed for the (1)GlcNAc residue of Fc wt correspond to two different conformations of the N-glycan. This seems unlikely because the peak intensity does not change upon altering the glycan composition, and it is known that glycan extension stabilizes the N-glycan (Barb, 2015; Barb et al., 2012). An alternative and potentially more likely possibility is that the two (1)GlcNAc Fc peaks result from exchange



of the nearby Y296 sidechain between two conformations as was observed by Kato and coworkers (Matsumiya et al., 2007). In either case, it is clear that multiple conformations of the C'E loop are found in Fc wt, and the presence of only the dominant conformation observed with Fc wt is consistent with efficient Fc $\gamma$ RIIIa binding.

### The behavior of the Fc D265A N-glycan termini is similar to Fc wt

If D265 is required for coordinating the C'E loop by binding the (1)GlcNAc residue, then we expect that removing the D265-mediated interaction will disrupt N-glycan/polypeptide interactions. F241 and F243 are known to contribute to N-glycan restriction (Lund et al., 1996; Subedi et al., 2014), but the relative importance of each glycan/polypeptide interface to C'E loop restriction and Fc $\gamma$ RIIIa binding is unclear. Evidence supporting a small disruption of the interface between N-glycan and polypeptide residues is found in an analysis of the glycans following expression of Fc D265A in the HEK293F cell line. MS analysis of purified N-glycans revealed a surprisingly small shift towards more highly modified glycoforms when compared to the Fc wt protein (Table S3) and is similar to mIgG2b Fc D265A (Baudino et al., 2008). However, the degree of glycan remodeling is still far less than that observed with other Fc variants. Fc F241S/F243S shows complete disruption of the N-glycan polypeptide interface and near complete glycan processing in the Golgi which is reflected in the recovery of glycans with high levels of galactose and sialic acid incorporation and the appearance of tri-antennary forms (Table S3 and (Subedi et al., 2014)). The effects of N-glycan heterogeneity are removed by enzymatic glycan remodeling *in vitro* prior to structural and functional characterization (Barb et al., 2009; Barb et al., 2012; Barb and Prestegard, 2011; Subedi et al., 2014).

Motion of the N-glycan termini can be measured by solution NMR spectroscopy. Previous studies reported a strong correlation between the position of peaks in 2D NMR spectra of terminal galactose residues and motion of the N-glycan termini (Barb et al., 2012; Barb and Prestegard, 2011; Subedi et al., 2014). The resonance frequency of the (6')galactose  $^{13}\text{C}$  nuclei represent a population-weighted average of the resonance frequencies of two distinct states: the predominant state *A* with the N-glycan terminus free from restriction and state *B* characterized by a direct interaction between the (6')galactose residue and K246 sidechain (Barb and Prestegard, 2011). The (6)galactose residue undergoes a similar change in states, but does not appear to directly contact the Fc polypeptide surface (Subedi et al., 2014). Thus, the more populated the unrestricted *A* state, the closer the observed resonance frequency is to the frequency of the same nucleus in an unrestricted N-glycan (labeled "e" in Fig 7).

A  $^1\text{H}$ - $^{13}\text{C}$  HSQC spectrum of ( $^{13}\text{C}$ -galactose-labeled)-Fc D265A, after enzymatic remodeling to the homogenous glycoform in Fig 1B, is remarkably similar to a spectrum of ( $^{13}\text{C}$ -galactose)-Fc wt as shown in Figure 7. The spectrum of Fc D265A shows minimal displacement towards the exposed state of the N-glycan, and a small increase in an unrestricted form (marked "e" in Fig 7). Based on previous results (Subedi et al., 2014), the displacement observed here indicates a small increase in the mobility of the N-glycan termini, and is consistent with the relatively small shift in glycan distribution noted at the beginning of this sub section. This result is remarkable because it indicates that the

interaction between the N-glycan termini and polypeptide is only marginally perturbed by the D265A mutation; the primary perturbation due to the D265A substitution is restricted to the C'E loop and is not largely transmitted along the length of the N-glycan to the branch termini. Thus, contacts proximal to the C'E loop contribute more to structural stabilization of the polypeptide conformation, and Fc $\gamma$ R11a affinity, than distal interactions between the N-glycan and polypeptide residues. Our observation is consistent with a published report on a different glycoprotein, CD2, indicating 2/3 of the stabilizing effect of an N-glycan on the underlying polypeptide is contributed by the (1)GlcNAc residue, and the remainder by the more distal residues (Hanson et al., 2009).

## Discussion

We previously reported that the intramolecular interface between the Fc N-glycan and polypeptide surface acts to modulate Fc $\gamma$ R11a affinity through allostery, however, the mechanism behind this allosteric modulation of Fc $\gamma$ R11a affinity was not defined (Subedi et al., 2014). The data presented herein clearly define the relationship between the structure and function of Fc N-glycosylation. Based on these results the primary role of the IgG1 Fc N-glycan is to stabilize the C'E loop through intramolecular interactions between carbohydrate and amino acid residues and, as a result, preorganize the Fc $\gamma$ R11a interface for optimal binding affinity.

The evidence supporting this conclusion includes solution-based studies of the Fc T299A and Fc D265A variants that reveal structural perturbations are restricted to the C'E loop (Fig 3–5). With Fc T299A, we found no difference in Fc quaternary structure upon comparison to Fc wt by measuring relative C $\gamma$ 2/C $\gamma$ 3 domain orientation (Fig 2). Furthermore, the C'E loop conformation shows a strong correlation with Fc $\gamma$ R11a affinity as measured through Y300 using Fc glycan and polypeptide variants (Fig 5). These data, combined with measurements of the N-glycan (Figs 6–7), indicate the N-glycan does not directly stabilize the optimal C $\gamma$ 2 orientation for Fc $\gamma$ R11a binding. A previous report implicates residues in the hinge region and at the C $\gamma$ 2/C $\gamma$ 3 domain interface as critical for determining C $\gamma$ 2 orientation (Frank et al., 2014).

We developed a model of Fc conformational states that incorporates the diversity of in vitro enzymecatalyzed modification results, solution-, and solid-state structural data (Fig 8). As determined above, the predominant solution conformation of Fc with a complex-type biantennary N-glycan is well represented by one structure from x-ray crystallography (1L6X) and is shown as state *iv*. This form is primed for Fc $\gamma$ R11a binding, upon which minor conformational adjustments may occur to form state *v*, a complex with Fc $\gamma$ R11a.

At the other extreme, Fc samples conformations that are not suitable for binding. It is known from a wealth of reports that the Fc N-glycan is fully exposed for modification by glycan-modifying enzymes (Barb et al., 2012; Barb and Prestegard, 2011; Kobata, 2008; Raju, 2008; Subedi et al., 2014; Yu et al., 2013). Two steps must occur before the N-glycan can become exposed if the dominant state is represented by *iv*. First, the N-glycan must detach from the surface of the protein. It was previously shown that the N-glycan termini are continuously exchanging between unrestricted and peptide bound forms (Barb and



Prestegard, 2011). Extensive 200 ns all-atom computational simulations indicate exchange of the glycan termini is largely a local event limited to a few angstroms of deviation (Frank et al., 2014). This event alone is likely insufficient to fully expose the N-glycans for enzymatic modification. Second, it is likely the C $\gamma$ 2 domains reorient to allow the N-glycans to become fully exposed. The wealth of Fc models point to a twisting motion of the C $\gamma$ 2 domain, though one model for a more dramatically altered conformation is proposed (Crispin et al., 2009).

Based on our analysis of Fc D265A, C'E loop deformation likely precedes N-glycan exposure. This is supported by the contact that is maintained between the Fc D265A N-glycan termini and polypeptide interface (Fig 7). On the other hand, one would expect a fully exposed Fc D265A N-glycan if N-glycan exposure precedes C'E loop deformation. We observed restriction, rather than complete exposure (Fig 7). Furthermore, it appears that conformational states with altered C'E loop conformation have preserved C $\gamma$ 2 domain orientation (Fig 2–5). The most likely pathway from state *iv* to state *i* (with a fully exposed N-glycan) goes through state *iii* with a disordered C'E loop, followed by C $\gamma$ 2 reorientation (represented by *ii*). It is also possible the order of these two events is reversed, as indicated by the alternate *iv* – *vi* – *ii* – *i* pathway.

The predominant contribution of C'E loop conformation to Fc $\gamma$ RIIIa affinity, and likely ADCC, highlights a pathway for rational mAb improvement. Protein engineering to stabilize the C'E loop in the conformation observed in Fc:Fc $\gamma$ RIIIa complexes and independent of glycosylation would benefit efficacy and reduce production cost if the N-glycan could be avoided entirely. These benefits are possible because the N-glycan exerts only an allosteric effect and is not known to directly contact receptors, if the designs prove to be tolerated by the patient immune system.

## Materials and Methods

### Materials

Materials were purchased from Sigma-Aldrich, unless otherwise noted. Fc wt and Fc polypeptide variants were prepared as previously described as well as all Fc glycovariants (Subedi et al., 2014), unless otherwise noted. All methods, including glycan analysis by MALDI-MS, were conducted as described (Subedi et al., 2014), unless otherwise noted.

### Protein expression

Human IgG1-Fc (residues 216–447) was largely prepared as described (Subedi et al., 2014) with a 25 residues trypanosome signal peptide (Vandersall-Nairn et al., 1998) appended to the N-terminus was cloned into the *NotI* and *HindIII* sites of the pGen2 vector (Barb et al., 2012). Plasmids encoding IgG1 Fc mutations were made according to the QuikChange method (Agilent Technologies). All mutations were confirmed by DNA sequencing (ISU DNA Facility). The extracellular region of Fc $\gamma$ RIIIa (residues 19–193, V158 allotype) containing N-terminal 8  $\times$  histidine and Green Fluorescent Protein (GFP) tags and a Tobacco etch virus (TEV) protease digestion site was cloned into the *EcoRI* and *HindIII*

sites of the pGen2 vector (Barb et al., 2012) and expressed according to previously described conditions (Subedi et al., 2014).

### Isotope-enriched Fc samples

[<sup>15</sup>N-Y/K] Fc was prepared as described (Subedi et al., 2014) except using custom FreeStyle293 expression medium (lacking tyrosine, lysine or phenylalanine) supplemented with [<sup>15</sup>N]-L-tyrosine, [<sup>15</sup>N]-L-lysine and unlabeled L-phenylalanine at 100 mg/L. <sup>13</sup>C<sub>U</sub> labeling of Fc glycans was achieved by using [<sup>13</sup>C<sub>U</sub>]-glucose as a metabolic precursor (Yamaguchi et al., 1998). Cells were transfected, diluted and cultured in FreeStyle2932122; medium as described (Subedi et al., 2014) except the medium was supplemented with 3 g/L [<sup>13</sup>C<sub>U</sub>]-glucose.

### NMR spectroscopy

NMR measurements were collected at 37–50°C using either a 700 MHz Bruker Avance II spectrometer or an 800 MHz Bruker Avance III spectrometer, both equipped with a 5 mm cryogenically cooled probe. Residual Dipolar Coupling (RDC) measurements were performed using [<sup>15</sup>N]-Tyr/Lys labeled IgG1 Fc samples. NMR samples were prepared in 20 mM MOPS, pH 7.4, 100 mM NaCl in a 10% D<sub>2</sub>O buffer. IgG1 Fc samples for anisotropic measurements were prepared by adding Pf1 phage (ASLA Biotech Ltd.) at a final concentration of 6–12 mg/ml in 210 µl with Fc protein up to 0.3–0.4 mM (dimer). NMR samples with Pf1 phage were mixed thoroughly and degassed by incubation at 50°C before the transfer to 4 mm Shigemi NMR tube. The <sup>2</sup>H splitting in the phage-included sample was observed between 4–10 Hz.

Isotropic (<sup>1</sup>J<sub>NH</sub>) and anisotropic (<sup>1</sup>J<sub>NH</sub> + <sup>1</sup>D<sub>NH</sub>) couplings to measure N-H bond residual dipolar coupling (RDCs) was observed using a heteronuclear single-quantum coherence (HSQC) transverse relaxation optimized spectroscopy (TROSY) based *J*-modulated pulse sequence (Liu and Prestegard, 2009). The modulation delays (ms) were 0.5, 1.0, 1.75, 3.5, 5.0, 6.5, 7.5 and 10.0. The number of scans used were between 48–80 with FID size of 2048 pts (<sup>1</sup>H) × 96 pts (<sup>15</sup>N). The isotropic and anisotropic measurements for each sample took approximately 24 h and 32 h, respectively. Spectra were processed using NMRpipe (Delaglio et al., 1995). Peak intensities were measured and *J*-modulation values fitted using NMRViewJ (One Moon Scientific, LLC). RDCs were used to calculate orientation tensors and Q values using PALES (Zweckstetter and Bax, 2000). Hydrogen atoms were added to Fc structures from the Protein Data Bank (Berman et al., 2002) using REDUCE (Word et al., 1999).

NMR measurements of amide <sup>15</sup>N *R*<sub>1</sub> and *R*<sub>2</sub> relaxation rates were collected on the 800 MHz spectrometer using HSQC-TROSY based methods available in the Bruker TopSpin 3.2 software package and analyzed using NMRViewJ. *R*<sub>1</sub> measurements were collected using 8 different relaxation delay periods (0.2, 0.4, 0.75, 1.0, 1.25, 1.5, 2.25 and 3 s) with a minimum 4.8–2 s delay between scans. *R*<sub>2</sub> measurements were collected using 7 different relaxation delay periods (4, 8, 12, 16, 20, 24 and 28 ms) with a 2 s delay between scans.

## Supplementary Material

Refer to Web version on PubMed Central for supplementary material.

## Acknowledgement

The authors thank Mr. Quinlin M. Hanson for preparing the D265A and T299A Fc variants, and Dr. D. Bruce Fulton of the Iowa State University Nuclear Magnetic Resonance Facility. This work was financially supported by the grant K22AI099165 from the National Institutes of Health, and by funds from the Roy J. Carver Department of Biochemistry, Biophysics & Molecular Biology at Iowa State University. The content of this work is solely the responsibility of the authors and does not necessarily represent the official views of the NIH.

## References

- Adams GP, Weiner LM. Monoclonal antibody therapy of cancer. *Nat Biotechnol.* 2005; 23:1147–1157. [PubMed: 16151408]
- Ahmed AA, Giddens J, Pincetic A, Lomino JV, Ravetch JV, Wang LX, Bjorkman PJ. Structural characterization of anti-inflammatory immunoglobulin G Fc proteins. *Journal of molecular biology.* 2014; 426:3166–3179. [PubMed: 25036289]
- Arnold JN, Wormald MR, Sim RB, Rudd PM, Dwek RA. The impact of glycosylation on the biological function and structure of human immunoglobulins. *Annu Rev Immunol.* 2007; 25:21–50. [PubMed: 17029568]
- Barb AW. Intramolecular N-Glycan/Polypeptide Interactions Observed at Multiple N-Glycan Remodeling Steps through [(13)C,(15)N]-N-Acetylglucosamine Labeling of Immunoglobulin G1. *Biochemistry.* 2015; 54:313–322. [PubMed: 25551295]
- Barb AW, Brady EK, Prestegard JH. Branch-specific sialylation of IgG-Fc glycans by ST6Gal-I. *Biochemistry.* 2009; 48:9705–9707. [PubMed: 19772356]
- Barb AW, Meng L, Gao Z, Johnson RW, Moremen KW, Prestegard JH. NMR characterization of immunoglobulin G Fc glycan motion on enzymatic sialylation. *Biochemistry.* 2012; 51:4618–4626. [PubMed: 22574931]
- Barb AW, Prestegard JH. NMR analysis demonstrates immunoglobulin G N-glycans are accessible and dynamic. *Nat Chem Biol.* 2011; 7:147–153. [PubMed: 21258329]
- Baruah K, Bowden TA, Krishna BA, Dwek RA, Crispin M, Scanlan CN. Selective deactivation of serum IgG: a general strategy for the enhancement of monoclonal antibody receptor interactions. *Journal of molecular biology.* 2012; 420:1–7. [PubMed: 22484364]
- Baudino L, Shinohara Y, Nimmerjahn F, Furukawa J, Nakata M, Martinez-Soria E, Petry F, Ravetch JV, Nishimura S, Izui S. Crucial role of aspartic acid at position 265 in the CH2 domain for murine IgG2a and IgG2b Fc-associated effector functions. *Journal of immunology.* 2008; 181:6664–6669.
- Berman HM, Battistuz T, Bhat TN, Bluhm WF, Bourne PE, Burkhardt K, Feng Z, Gilliland GL, Iype L, Jain S, et al. The Protein Data Bank. *Acta Crystallogr D Biol Crystallogr.* 2002; 58:899–907. [PubMed: 12037327]
- Borrok MJ, Jung ST, Kang TH, Monzingo AF, Georgiou G. Revisiting the role of glycosylation in the structure of human IgG Fc. *ACS chemical biology.* 2012; 7:1596–1602. [PubMed: 22747430]
- Bournazos S, Klein F, Pietzsch J, Seaman MS, Nussenzweig MC, Ravetch JV. Broadly neutralizing anti-HIV-1 antibodies require Fc effector functions for in vivo activity. *Cell.* 2014; 158:1243–1253. [PubMed: 25215485]
- Bruhns P, Iannascoli B, England P, Mancardi DA, Fernandez N, Jorieux S, Daeron M. Specificity and affinity of human Fcγ receptors and their polymorphic variants for human IgG subclasses. *Blood.* 2009; 113:3716–3725. [PubMed: 19018092]
- Cavanagh J, Fairbrother WJ, Palmer AG, Rance M, Skelton NJ. *Protein NMR Spectroscopy: Principles and Practice, 2nd Edition.* Protein Nmr Spectroscopy: Principles and Practice (2nd Edition). 2007:1–888.
- Chadd HE, Chamow SM. Therapeutic antibody expression technology. *Curr Opin Biotechnol.* 2001; 12:188–194. [PubMed: 11287236]

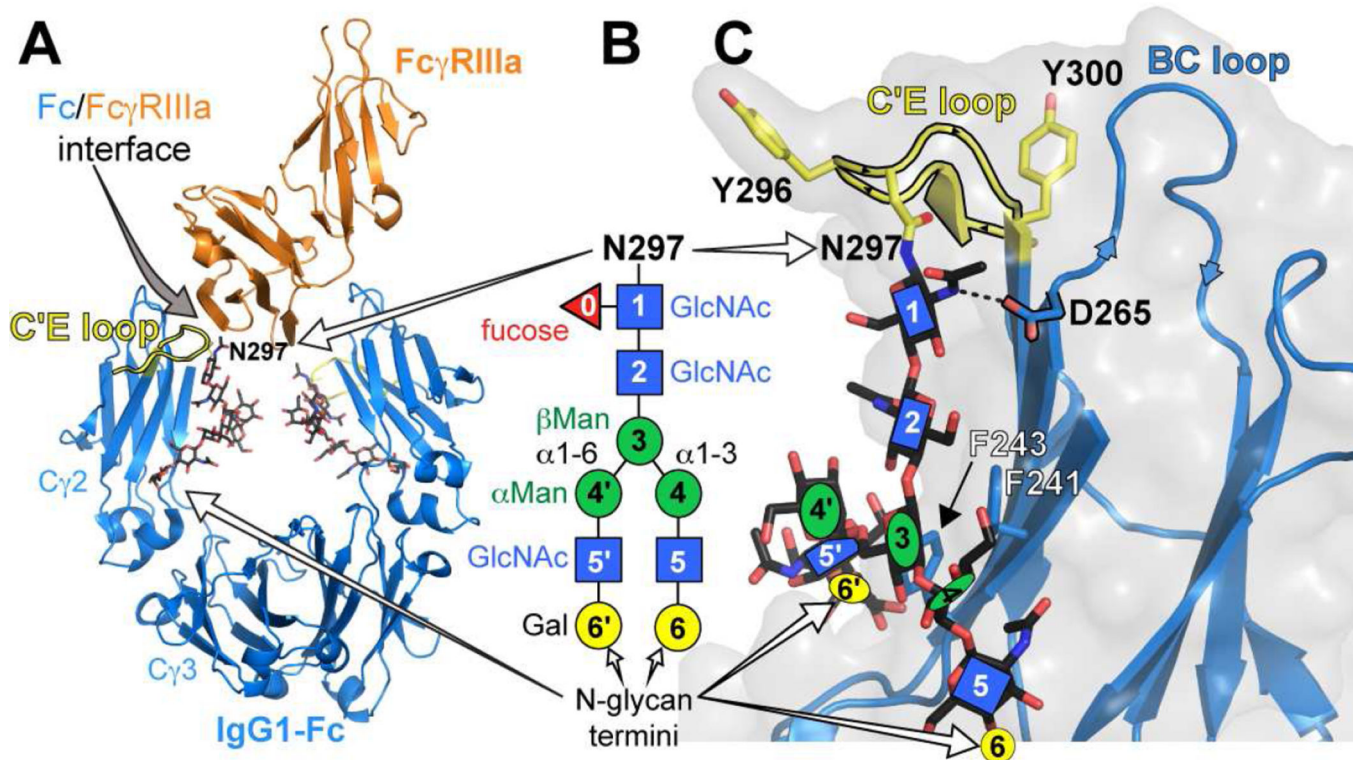
- Chan AC, Carter PJ. Therapeutic antibodies for autoimmunity and inflammation. *Nat Rev Immunol*. 2010; 10:301–316. [PubMed: 20414204]
- Clynes RA, Towers TL, Presta LG, Ravetch JV. Inhibitory Fc receptors modulate in vivo cytotoxicity against tumor targets. *Nature medicine*. 2000; 6:443–446.
- Cornilescu G, Marquardt JL, Ottiger M, Bax A. Validation of protein structure from anisotropic carbonyl chemical shifts in a dilute liquid crystalline phase. *Journal of the American Chemical Society*. 1998; 120:6836–6837.
- Crispin M, Bowden TA, Coles CH, Harlos K, Aricescu AR, Harvey DJ, Stuart DI, Jones EY. Carbohydrate and domain architecture of an immature antibody glycoform exhibiting enhanced effector functions. *Journal of molecular biology*. 2009; 387:1061–1066. [PubMed: 19236877]
- Crispin M, Yu X, Bowden TA. Crystal structure of sialylated IgG Fc: implications for the mechanism of intravenous immunoglobulin therapy. *Proc Natl Acad Sci U S A*. 2013; 110:E3544–E3546. [PubMed: 23929778]
- Deisenhofer J. Crystallographic refinement and atomic models of a human Fc fragment and its complex with fragment B of protein A from *Staphylococcus aureus* at 2.9- and 2.8-Å resolution. *Biochemistry*. 1981; 20:2361–2370. [PubMed: 7236608]
- Delaglio F, Grzesiek S, Vuister GW, Zhu G, Pfeifer J, Bax A. NMRPipe: a multidimensional spectral processing system based on UNIX pipes. *Journal of biomolecular NMR*. 1995; 6:277–293. [PubMed: 8520220]
- DeLano WL, Ultsch MH, de Vos AM, Wells JA. Convergent solutions to binding at a protein-protein interface. *Science*. 2000; 287:1279–1283. [PubMed: 10678837]
- Farmer BT 2nd, Constantine KL, Goldfarb V, Friedrichs MS, Wittekind M, Yanchunas J Jr, Robertson JG, Mueller L. Localizing the NADP<sup>+</sup> binding site on the MurB enzyme by NMR. *Nat Struct Biol*. 1996; 3:995–997. [PubMed: 8946851]
- Feige MJ, Nath S, Catharino SR, Weinfurter D, Steinbacher S, Buchner J. Structure of the murine unglycosylated IgG1 Fc fragment. *Journal of molecular biology*. 2009; 391:599–608. [PubMed: 19559712]
- Ferrara C, Grau S, Jager C, Sondermann P, Brunker P, Waldhauer I, Hennig M, Ruf A, Rufer AC, Stihle M, et al. Unique carbohydrate-carbohydrate interactions are required for high affinity binding between Fcγ<sub>3</sub> and antibodies lacking core fucose. *Proc Natl Acad Sci U S A*. 2011; 108:12669–12674. [PubMed: 21768335]
- Frank M, Walker RC, Lanzilotta WN, Prestegard JH, Barb AW. Immunoglobulin G1 Fc domain motions: implications for Fc engineering. *Journal of molecular biology*. 2014; 426:1799–1811. [PubMed: 24522230]
- Franklin EC. Structure and function of immunoglobulins. *Acta Endocrinol Suppl (Copenh)*. 1975; 194:77–95. [PubMed: 47690]
- Gavel Y, von Heijne G. Sequence differences between glycosylated and non-glycosylated Asn-X-Thr/Ser acceptor sites: implications for protein engineering. *Protein Eng*. 1990; 3:433–442. [PubMed: 2349213]
- Hanson SR, Culyba EK, Hsu TL, Wong CH, Kelly JW, Powers ET. The core trisaccharide of an N-linked glycoprotein intrinsically accelerates folding and enhances stability. *Proc Natl Acad Sci U S A*. 2009; 106:3131–3136. [PubMed: 19204290]
- Huber R, Deisenhofer J, Colman PM, Matsushima M, Palm W. Crystallographic structure studies of an IgG molecule and an Fc fragment. *Nature*. 1976; 264:415–420. [PubMed: 1004567]
- Ishima R, Torchia DA. Protein dynamics from NMR. *Nat Struct Biol*. 2000; 7:740–743. [PubMed: 10966641]
- Jaffe SR, Strutton B, Levarski Z, Pandhal J, Wright PC. *Escherichia coli* as a glycoprotein production host: recent developments and challenges. *Curr Opin Biotechnol*. 2014; 30:205–210. [PubMed: 25156401]
- Janeway, C.; Murphy, KP.; Travers, P.; Walport, M. *Janeway's immuno biology*. 7th edn. New York: Garland Science; 2008.
- Jefferis R. Recombinant antibody therapeutics: the impact of glycosylation on mechanisms of action. *Trends in pharmacological sciences*. 2009; 30:356–362. [PubMed: 19552968]

- Jefferis R, Lund J, Pound JD. IgG-Fc-mediated effector functions: molecular definition of interaction sites for effector ligands and the role of glycosylation. *Immunol Rev.* 1998; 163:59–76. [PubMed: 9700502]
- Jiang XR, Song A, Bergelson S, Arroll T, Parekh B, May K, Chung S, Strouse R, Mire-Sluis A, Schenerman M. Advances in the assessment and control of the effector functions of therapeutic antibodies. *Nat Rev Drug Discov.* 2011; 10:101–111. [PubMed: 21283105]
- Kaneko Y, Nimmerjahn F, Ravetch JV. Anti-inflammatory activity of immunoglobulin G resulting from Fc sialylation. *Science.* 2006; 313:670–673. [PubMed: 16888140]
- Kato K, Yamaguchi Y, Arata Y. Stable-isotope-assisted NMR approaches to glycoproteins using immunoglobulin G as a model system. *Prog Nucl Magn Reson Spectrosc.* 2010; 56:346–359. [PubMed: 20633358]
- Kobata A. The N-linked sugar chains of human immunoglobulin G: their unique pattern, and their functional roles. *Biochim Biophys Acta.* 2008; 1780:472–478. [PubMed: 17659840]
- Krapp S, Mimura Y, Jefferis R, Huber R, Sondermann P. Structural analysis of human IgG-Fc glycoforms reveals a correlation between glycosylation and structural integrity. *Journal of molecular biology.* 2003; 325:979–989. [PubMed: 12527303]
- Lazar GA, Chirino AJ, Dang W, Desjarlais JR, Doberstein SK, Hayes RJ, Karki SBaVO. Optimized Fc variants and methods for their generation. 2009
- Lindorff-Larsen K, Best RB, Depristo MA, Dobson CM, Vendruscolo M. Simultaneous determination of protein structure and dynamics. *Nature.* 2005; 433:128–132. [PubMed: 15650731]
- Liu Y, Prestegard JH. Measurement of one and two bond N-C couplings in large proteins by TROSY-based J-modulation experiments. *Journal of magnetic resonance.* 2009; 200:109–118. [PubMed: 19581113]
- Lund J, Takahashi N, Pound JD, Goodall M, Jefferis R. Multiple interactions of IgG with its core oligosaccharide can modulate recognition by complement and human Fc gamma receptor I and influence the synthesis of its oligosaccharide chains. *Journal of immunology.* 1996; 157:4963–4969.
- Lund J, Takahashi N, Pound JD, Goodall M, Nakagawa H, Jefferis R. Oligosaccharide-protein interactions in IgG can modulate recognition by Fc gamma receptors. *FASEB J.* 1995; 9:115–119. [PubMed: 7821750]
- Lux A, Yu X, Scanlan CN, Nimmerjahn F. Impact of immune complex size and glycosylation on IgG binding to human Fc gammaRs. *Journal of immunology.* 2013; 190:4315–4323.
- Matsumiya S, Yamaguchi Y, Saito J, Nagano M, Sasakawa H, Otaki S, Satoh M, Shitara K, Kato K. Structural comparison of fucosylated and nonfucosylated Fc fragments of human immunoglobulin G1. *Journal of molecular biology.* 2007; 368:767–779. [PubMed: 17368483]
- Mertens HD, Svergun DI. Structural characterization of proteins and complexes using small-angle X-ray solution scattering. *J Struct Biol.* 2010; 172:128–141. [PubMed: 20558299]
- Mimura Y, Sondermann P, Ghirlando R, Lund J, Young SP, Goodall M, Jefferis R. Role of oligosaccharide residues of IgG1-Fc in Fc gamma RIIb binding. *J Biol Chem.* 2001; 276:45539–45547. [PubMed: 11567028]
- Mittermaier A, Kay LE. New tools provide new insights in NMR studies of protein dynamics. *Science.* 2006; 312:224–228. [PubMed: 16614210]
- Mizuochi T, Taniguchi T, Shimizu A, Kobata A. Structural and numerical variations of the carbohydrate moiety of immunoglobulin G. *Journal of immunology.* 1982; 129:2016–2020.
- Mizushima T, Yagi H, Takemoto E, Shibata-Koyama M, Isoda Y, Iida S, Masuda K, Satoh M, Kato K. Structural basis for improved efficacy of therapeutic antibodies on defucosylation of their Fc glycans. *Genes to cells : devoted to molecular & cellular mechanisms.* 2011; 16:1071–1080. [PubMed: 22023369]
- Nimmerjahn F, Ravetch JV. Fc gamma receptors as regulators of immune responses. *Nat Rev Immunol.* 2008; 8:34–47. [PubMed: 18064051]
- Nisonoff A, Wissler FC, Lipman LN, Woernley DL. Separation of univalent fragments from the bivalent rabbit antibody molecule by reduction of disulfide bonds. *Arch Biochem Biophys.* 1960; 89:230–244. [PubMed: 14427334]

- Nose M, Wigzell H. Biological significance of carbohydrate chains on monoclonal antibodies. *Proc Natl Acad Sci U S A*. 1983; 80:6632–6636. [PubMed: 6579549]
- Porter RR. The hydrolysis of rabbit  $\gamma$ -globulin and antibodies with crystalline papain. *Biochem J*. 1959; 73:119–126. [PubMed: 14434282]
- Prestegard JH, Agard DA, Moremen KW, Lavery LA, Morris LC, Pederson K. Sparse labeling of proteins: structural characterization from long range constraints. *Journal of magnetic resonance*. 2014; 241:32–40. [PubMed: 24656078]
- Raju TS. Terminal sugars of Fc glycans influence antibody effector functions of IgGs. *Curr Opin Immunol*. 2008; 20:471–478. [PubMed: 18606225]
- Religa TL, Sprangers R, Kay LE. Dynamic regulation of archaeal proteasome gate opening as studied by TROSY NMR. *Science*. 2010; 328:98–102. [PubMed: 20360109]
- Roque AC, Lowe CR, Taipa MA. Antibodies and genetically engineered related molecules: production and purification. *Biotechnol Prog*. 2004; 20:639–654. [PubMed: 15176864]
- Sazinsky SL, Ott RG, Silver NW, Tidor B, Ravetch JV, Wittrup KD. Aglycosylated immunoglobulin G1 variants productively engage activating Fc receptors. *Proc Natl Acad Sci U S A*. 2008; 105:20167–20172. [PubMed: 19074274]
- Scallon BJ, Tam SH, McCarthy SG, Cai AN, Raju TS. Higher levels of sialylated Fc glycans in immunoglobulin G molecules can adversely impact functionality. *Mol Immunol*. 2007; 44:1524–1534. [PubMed: 17045339]
- Scott AM, Wolchok JD, Old LJ. Antibody therapy of cancer. *Nat Rev Cancer*. 2012; 12:278–287. [PubMed: 22437872]
- Sethuraman N, Stadheim TA. Challenges in therapeutic glycoprotein production. *Curr Opin Biotechnol*. 2006; 17:341–346. [PubMed: 16828275]
- Siberil S, Dutertre CA, Fridman WH, Teillaud JL. Fc $\gamma$ R: The key to optimize therapeutic antibodies? *Crit Rev Oncol Hematol*. 2007; 62:26–33. [PubMed: 17240158]
- Silva-Martin N, Bartual SG, Ramirez-Aportela E, Chacon P, Park CG, Hermoso JA. Structural basis for selective recognition of endogenous and microbial polysaccharides by macrophage receptor SIGN-R1. *Structure*. 2014; 22:1595–1606. [PubMed: 25450767]
- Singh N, Pirsch J, Samaniego M. Antibody-mediated rejection: treatment alternatives and outcomes. *Transplant Rev (Orlando)*. 2009; 23:34–46. [PubMed: 19027615]
- Sliwkowski MX, Mellman I. Antibody therapeutics in cancer. *Science*. 2013; 341:1192–1198. [PubMed: 24031011]
- Sondermann P. Crystal Structures of Human IgG-Fc Fragments and Their Complexes with Fc $\gamma$  Receptors. In: Nimmerjahn, F., editor. *Molecular and Cellular Mechanisms of Antibody Activity*. New York: Springer Science+Business Media; 2013. p. 61-83.
- Sondermann P, Huber R, Oosthuizen V, Jacob U. The 3.2-A crystal structure of the human IgG1 Fc fragment-Fc  $\gamma$ III complex. *Nature*. 2000; 406:267–273. [PubMed: 10917521]
- Subedi GP, Hanson QM, Barb AW. Restricted motion of the conserved immunoglobulin G1 N-glycan is essential for efficient Fc $\gamma$ IIIa binding. *Structure*. 2014; 22:1478–1488. [PubMed: 25199692]
- Sutton BJ, Phillips DC. The three-dimensional structure of the carbohydrate within the Fc fragment of immunoglobulin G. *Biochem Soc Trans*. 1983; 11(Pt 2):130–132.
- Tugarinov V, Hwang PM, Kay LE. Nuclear magnetic resonance spectroscopy of high-molecular-weight proteins. *Annu Rev Biochem*. 2004; 73:107–146. [PubMed: 15189138]
- Tugarinov V, Kanelis V, Kay LE. Isotope labeling strategies for the study of high-molecular-weight proteins by solution NMR spectroscopy. *Nat Protoc*. 2006; 1:749–754. [PubMed: 17406304]
- Vandersall-Nairn AS, Merkle RK, O'Brien K, Oeltmann TN, Moremen KW. Cloning, expression, purification, and characterization of the acid  $\alpha$ -mannosidase from *Trypanosoma cruzi*. *Glycobiology*. 1998; 8:1183–1194. [PubMed: 9858640]
- Varki, A. *Essentials of glycobiology*. 2nd edn. Cold Spring Harbor, N.Y.: Cold Spring Harbor Laboratory Press; 2009.



- Word JM, Lovell SC, Richardson JS, Richardson DC. Asparagine and glutamine: Using hydrogen atom contacts in the choice of side-chain amide orientation. *Journal of molecular biology*. 1999; 285:1735–1747. [PubMed: 9917408]
- Yagi H, Zhang Y, Yagi-Utsumi M, Yamaguchi T, Iida S, Yamaguchi Y, Kato K, Backbone H, C, and N resonance assignments of the Fc fragment of human immunoglobulin G glycoprotein. *Biomolecular NMR assignments*. 2014
- Yamaguchi Y, Kato K, Shindo M, Aoki S, Furusho K, Koga K, Takahashi N, Arata Y, Shimada I. Dynamics of the carbohydrate chains attached to the Fc portion of immunoglobulin G as studied by NMR spectroscopy assisted by selective C-13 labeling of the glycans. *Journal of biomolecular NMR*. 1998; 12:385–394. [PubMed: 9835046]
- Yamaguchi Y, Nishimura M, Nagano M, Yagi H, Sasakawa H, Uchida K, Shitara K, Kato K. Glycoform-dependent conformational alteration of the Fc region of human immunoglobulin G1 as revealed by NMR spectroscopy. *Biochimica Et Biophysica Acta-General Subjects*. 2006; 1760:693–700.
- Yu X, Baruah K, Harvey DJ, Vasiljevic S, Alonzi DS, Song BD, Higgins MK, Bowden TA, Scanlan CN, Crispin M. Engineering hydrophobic protein-carbohydrate interactions to fine-tune monoclonal antibodies. *Journal of the American Chemical Society*. 2013; 135:9723–9732. [PubMed: 23745692]
- Zweckstetter M, Bax A. Prediction of sterically induced alignment in a dilute liquid crystalline phase: Aid to protein structure determination by NMR. *Journal of the American Chemical Society*. 2000; 122:3791–3792.

**Figure 1.**

Structure of the IgG1 Fc / Fc $\gamma$ RIIIa complex. **(A)** The IgG1 Fc dimer (*blue ribbon*) binds to the extracellular domain of Fc $\gamma$ RIIIa (*orange ribbon*) with high nM affinity. A substantial contact interface is formed by the C'E loop of one Fc chain (highlighted in *yellow*) and the receptor polypeptide. **(B)** The IgG Fc N-glycan, shown here in a cartoon diagram according to the CfG convention (Varki, 2009), is required for Fc $\gamma$ RIIIa binding. Numbers in the cartoon shapes represent the numbering strategy used to describe individual N-glycan residues. **(C)** The motion of the Fc N-glycan is restricted by contacts with the polypeptide surface, including F241, F243 and D265.

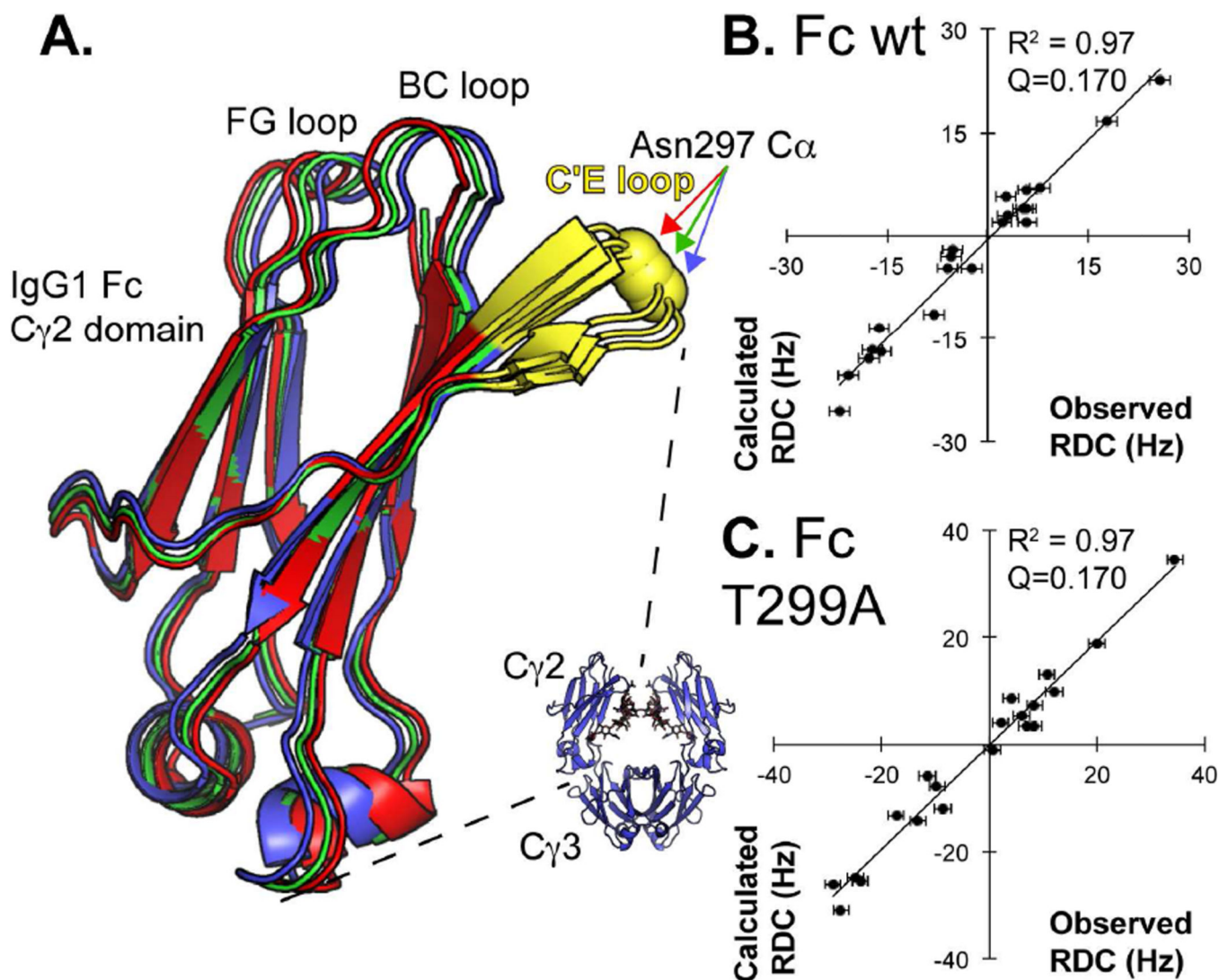


**Figure 2.**

NMR indicates that Fc wt C $\gamma$ 2 domain orientation, relative to the C $\gamma$ 3 domain, is nearly identical to that observed by x-ray crystallography and changes little upon removing the N-glycan. (A) Orientations of the C $\gamma$ 2 domains are overlaid following optimization of the C $\gamma$ 2 orientation, alignment of the C $\gamma$ 3 domains (not shown) and centering C $\gamma$ 2 domains by their centers of mass. The Fc model solved by x-ray crystallography is shown as a *blue* ribbon. The orientations of Fc wt in solution (*red* ribbon) and the non-glycosylated variant Fc T299A (*green* ribbon) are also shown. Comparisons to the observed versus calculated RDCs for Fc wt and Fc T299A are shown in (B) and (C). The Fc N-glycan is not shown.

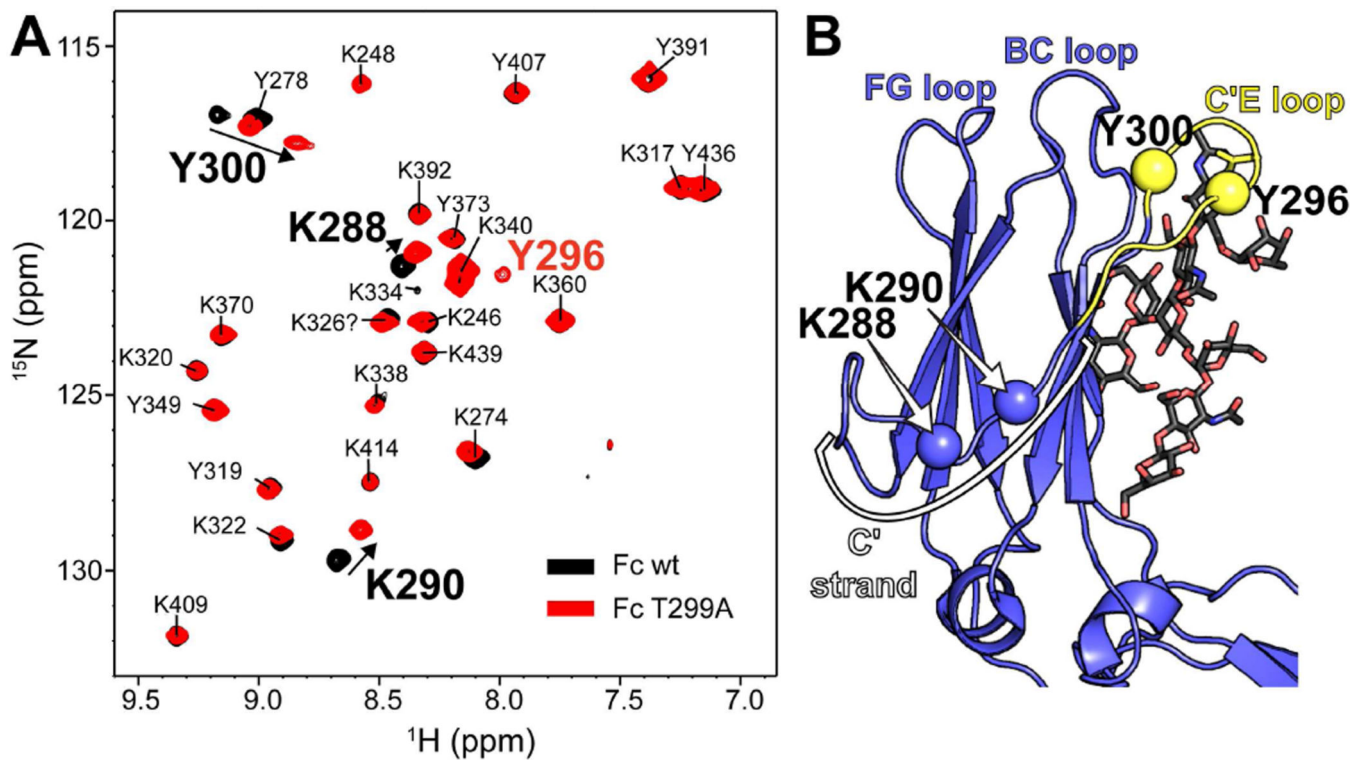


**Figure 3.**

A  $^1\text{H}$ - $^{15}\text{N}$ -HSQC TROSY spectrum reveals that N-glycan removal (with a T299A mutation) perturbs resonances in the C'E loop (Y296 & 300) and along the C' strand (K288 and K290). (A) These four resonances are found on the same structural feature as the N297 glycosylation site. (B) Y296 was not observed in spectra of glycosylated Fc wt. Fc assignments were reported by Kato and coworkers (Yagi et al., 2014).

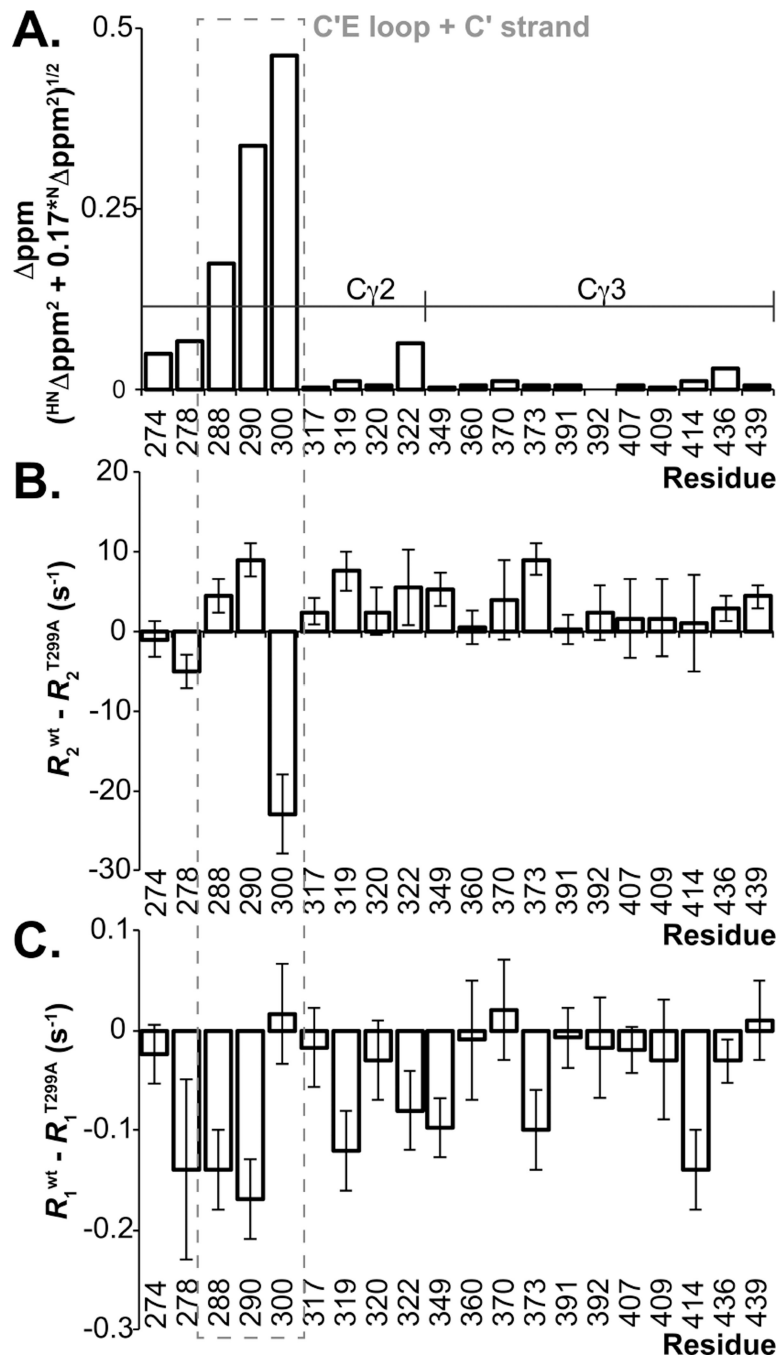


**Figure 4.** NMR measurements indicate C'E loop structure and motion is stabilized on the microsecond-millisecond timescale by N297 glycosylation. (A) Differences between peak positions of IgG1 Fc wt and the T299A variant are plotted as described (Farmer et al., 1996). The differences between backbone amide nitrogen relaxation rates from IgG1 Fc wt and the T299A variant measured using (B)  $R_2$  and (C)  $R_1$  experiments are shown. Error bars indicate the precision of measurement for each set of relaxation rates ( $\pm 1$  SD).



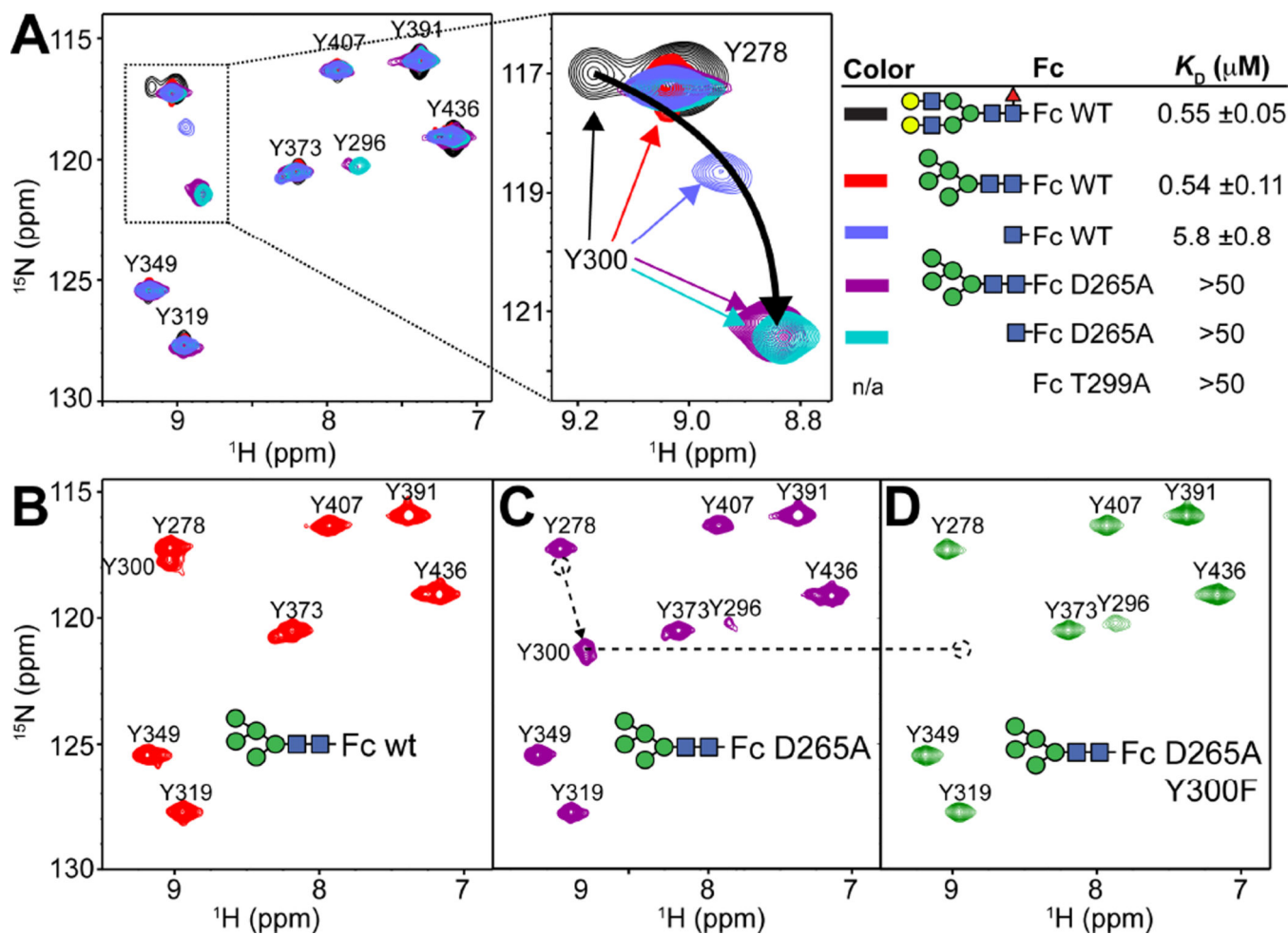


**Figure 5.**

The peak corresponding to Y300 is displaced in spectra of Fc variants. (A)  $^1\text{H}$ - $^{15}\text{N}$  HSQC-TROSY spectra of [ $^{15}\text{N}$ -Y]-Fc and Fc $\gamma$ RIIIa affinity of Fc variants. The *curved black arrow* shows the direction of chemical shift change of the Y300 peak with decreasing Fc $\gamma$ RIIIa affinity. (B) Assignment of the Y300 residue in Fc D265A spectrum was performed by comparison with a spectrum of the Fc Y300F/D265A variant.



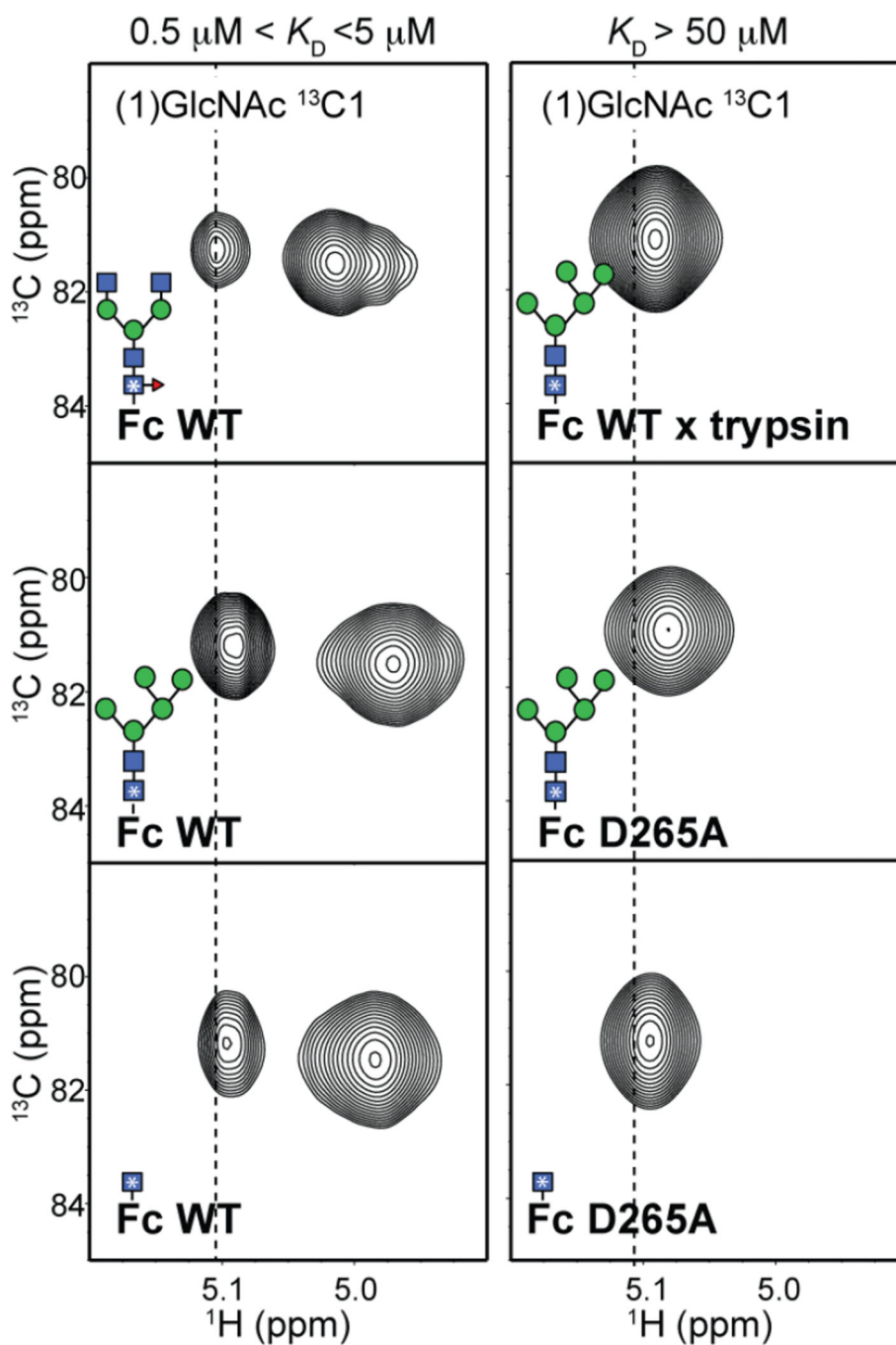


**Figure 6.**

The (1)GlcNAc residue experiences multiple chemical environments in Fc wt, but only one state is present in proteolyzed Fc or Fc variants that bind Fc $\gamma$ RIIIa weakly ( $>50 \mu\text{M}$ ).  $^1\text{H}$ - $^{13}\text{C}$  HSQC spectra of  $^{13}\text{C}$ -labeled Fc variants are drawn to highlight the spectral region corresponding to the anomeric region of the (1)GlcNAc residue. The vertical dashed line corresponds to the  $^1\text{H}$  chemical shift of the upfield signal in the Fc wt protein with a complex-type N-glycan. A complete spectrum of the Fc samples is shown in Supplemental Figure 6.

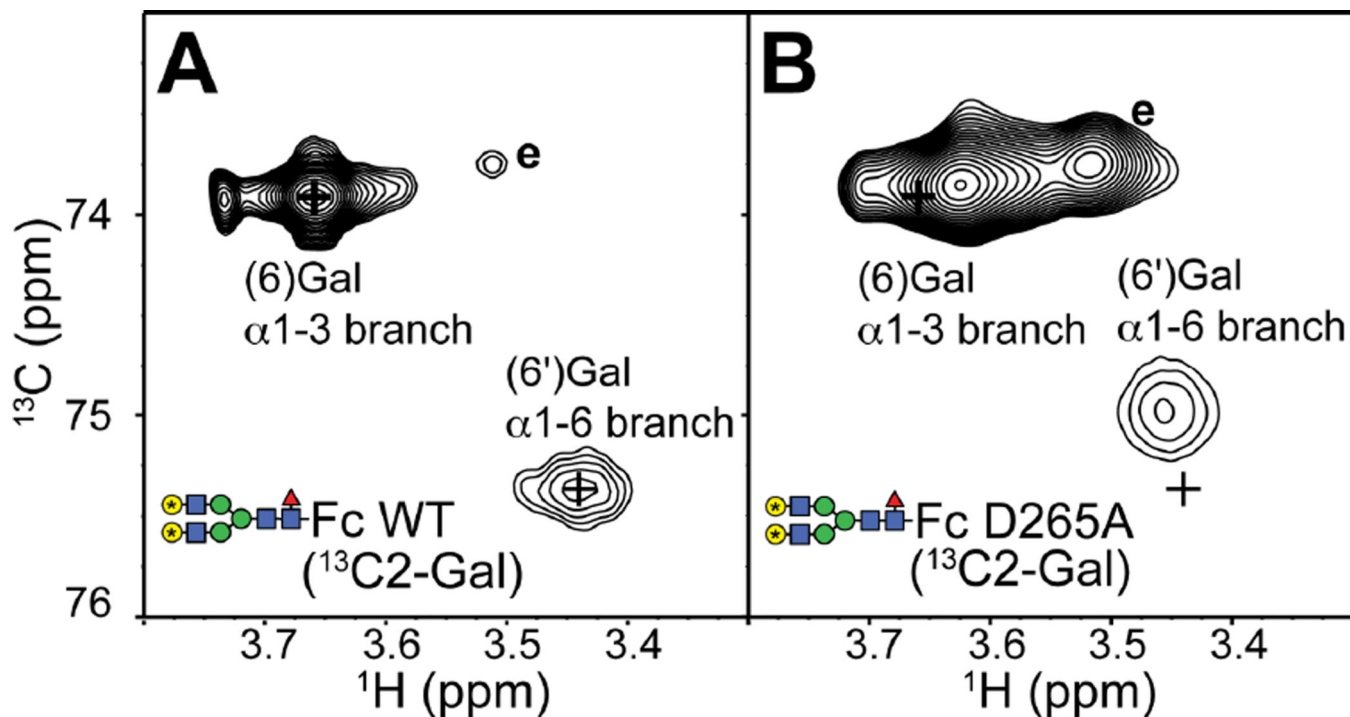


**Figure 7.** The D265A Fc variant retains significant contact between the polypeptide and N-glycan termini as observed with the (6) and (6') galactose residues.  $^1\text{H}$ - $^{13}\text{C}$  HSQC spectra of (A) IgG1 Fc wt and (B) D265A variant. N-glycans were remodeled to display the G2F glycoform with  $^{13}\text{C}_2$ -galactose. Positions of Fc wt peaks are highlighted by "+". Resonance frequencies consistent with an exposed and unrestricted N-glycan are labeled "e" (Subedi et al., 2014).

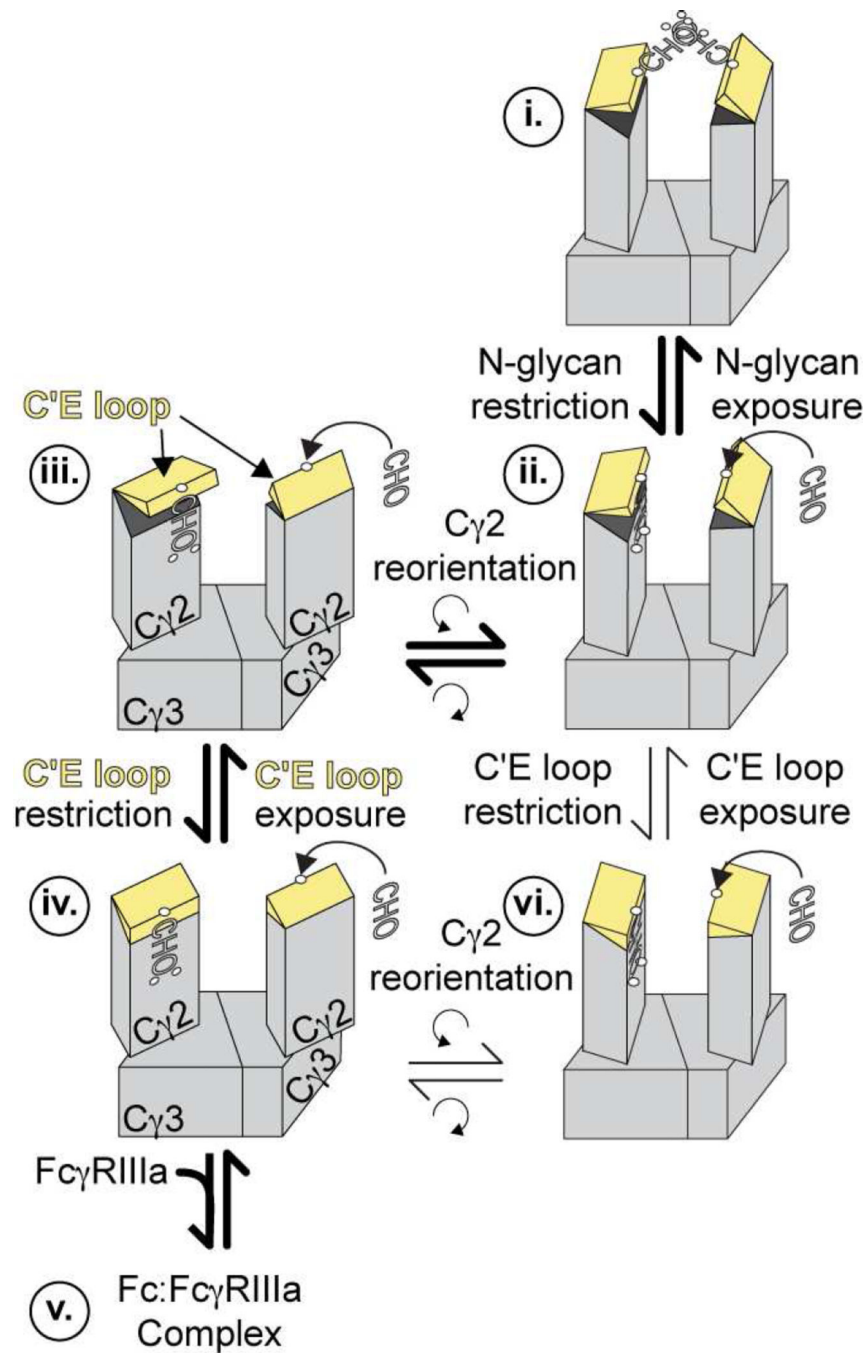


**Figure 8.** A comprehensive model of Fc conformations. The Fc N-glycan is required to restrict the C'E loop, and state *iv* represents the dominant conformation of Fc wt that is also predisposed to bind Fc $\gamma$ RIIIa. The equilibrium established between states *iii* and *iv* can be perturbed by removing the N-glycan or perturbing the N-glycan interface. For complete exposure of the N-glycan, known to occur based on the sensitivity to glycan modifying enzymes that bind

carbohydrate motifs consisting of 6+ residues, the C $\gamma$ 2 reorients to allow for complete dissociation of the N-glycan from the polypeptide surface and the Fc interstitial space.

Author Manuscript

Author Manuscript

Author Manuscript

Author Manuscript

**Table 1**IgG1 Fc wt RDCs fitted to PDB models (chain A<sup>1</sup>)

PDB ID	Q value from raw PDB	Q value after modeling PDB domain orientation with C $\gamma$ 2 and C $\gamma$ 3 from 1L6X	ref	notes
1L6X	<b>0.185</b>	n.a. <sup>2</sup>	(DeLano et al., 2000)	Fc + Z domain
2DTS	0.217	0.217	(Matsumiya et al., 2007)	afucosylated
4KU1	0.252	0.260	(Frank et al., 2014)	G2F
4BYH	0.270	0.226	(Crispin et al., 2013)	disialyl
2WAH	0.306	0.295	(Crispin et al., 2009)	M9N2
3AVE	0.306	0.218	(Matsumiya et al., 2007)	fucosylated
3AY4	0.308	0.183	(Mizushima et al., 2011)	afucosylated Fc + Fc $\gamma$ R11A
3DNK	0.355	0.210	unpublished	aglycosylated
3S7G	0.384	0.231	unpublished	aglycosylated
4Q6Y	0.397	0.268	(Ahmed et al., 2014)	disialyl
1H3T	0.404	0.221	(Krapp et al., 2003)	MN2F
1H3U	0.434	0.211	(Krapp et al., 2003)	M3N2F
4ACP	0.434	0.279	(Baruah et al., 2012)	EndoS treated
1E4K	0.438	0.207	(Sondermann et al., 2000)	Fc + Fc $\gamma$ R11A
1H3X	0.463	0.220	(Krapp et al., 2003)	G0F
1H3Y	0.488	0.230	(Krapp et al., 2003)	high salt
3DO3	0.496	0.230	unpublished	
1H3V	0.537	0.220	(Krapp et al., 2003)	G2F, P2 <sub>1</sub> 2 <sub>1</sub> 2 <sub>1</sub>
1FC1	0.542	0.207	(Deisenhofer, 1981)	
1H3W	0.561	0.189	(Krapp et al., 2003)	G2F, C222 <sub>1</sub>
3HKF	0.909	0.285	(Feige et al., 2009)	murine; aglycosylated
4CDH	n.d. <sup>3</sup>	0.225	(Silva-Martin et al., 2014)	disialyl

<sup>1</sup> fits to other polypeptides in the structure files, where available, provided similar results

<sup>2</sup> n.a.- not applicable

<sup>3</sup> n.d.- not determined; PALES failed to converge on a solution